

# Autonomous maneuver of a farm vehicle with a trailed implement: motion planner and lateral-longitudinal controllers

Christophe Cariou\*, Roland Lenain\*, Benoit Thuilot†, Philippe Martinet†

\* Cemagref

† LASMEA

24, av. des Landais

24, av. des Landais

63172 Aubière Cedex France

63177 Aubière Cedex France

christophe.cariou@cemagref.fr

benoit.thuilot@lasmea.univ-bpclermont.fr

**Abstract**—This paper addresses the problem of path generation and motion control for the autonomous maneuver of a farm vehicle with a trailed implement in headland. A reverse turn planner is firstly investigated, based on primitives connected together to easily generate the reference motion. Then, both steering and speed control algorithms are presented to accurately guide the vehicle-trailer system. They are based on a kinematic model extended with additional sliding parameters and on model predictive control approaches. Real world experiments have been carried out on a low friction terrain with an experimental mobile robot pulling a trailer. At the end of each row, the reverse turn is automatically generated to connect the next reference track, and the maneuver is autonomously performed by the vehicle-trailer system. Reported experiments demonstrate the capabilities of the proposed algorithms.

## I. INTRODUCTION

In the last few years, automatic guidance of agricultural vehicles has received increased interest to improve field efficiency, while releasing human operator from monotonous and dangerous operations, and recently to contribute to environmentally sustainable agricultural productions, see [7] and [12]. Many experiments have been conducted and reported in the literature, with numerous auto-steering systems marketed for semi-autonomous tractors (e.g. *Agco AutoGuide*, *Agrocom E-drive*, *Autofarm AutoSteer*, *Case IH AccuGuide*, *John-Deere AutoTrac*, *New-Holland IntelliSteer*). However, most of these researches focus on accurately following parallel tracks in the field, and seldom consider the maneuvers at the end of each row, still manually performed, all the more if steering backward a trailed implement is needed. In order to benefit of fully automated solutions, and therefore reduce the operator's workload (and even enable to consider driveless agricultural vehicles), the problem of maneuvers automation in headlands has to be studied with meticulous care.

Very few approaches have been proposed in that way, mainly based on loop turns (e.g. *John-Deere iTEC Pro*, see figure 1(a)). The drawback of such an approach is that it involves excessive headland width for turning on the adjacent track, all the more if a long trailer is used, and is thereby far from optimal in term of productivity, headland being usually low-yield field areas due to high soil compaction. A more efficient solution is to perform reverse turns, i.e. maneuvers executed with stop points and a reverse motion. In our previous work [2], fish-tail maneuvers, as highlighted in figure 1(b), were autonomously performed, in the case of a

self-propelled vehicle or a tractor with mounted implement. This type of maneuver leads to reduced headlands and is more in accordance with European agricultural practices. This paper proposes to extend this work considering a trailed implement hooked up at some distance from the middle point of the rear axle of the farm vehicle (i.e. the general 1-trailer system), leading to the maneuver depicted in figure 1(c). The automation of such a maneuver is a challenging problem in both path planning and control points of view. In particular, steering a vehicle-trailer system backward has a tendency to jackknife. Moreover, as pointed out in [17], wheel skidding and sliding are inevitable in an agricultural context and may seriously damage the accuracy of path tracking. Delays induced by steering and speed actuators may also lead to transient lateral overshoots when the vehicle enters into curves, or longitudinal overshoots when it stops.

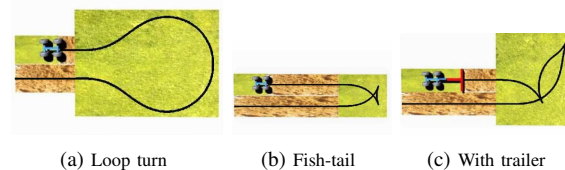


Fig. 1. Different types of maneuver in headland

In the literature, numerous approaches have been proposed for the control of a vehicle with one or several trailers, see for example [1], [14]. However, most of these control algorithms are devoted to road applications and seem not well-adapted for an agricultural context. For example, [8] has considered the trailer as a virtual robot for the backward motion, and has proposed a control law based on the idea that the linear and angular velocities of the vehicle and the trailer are connected by a one-to-one mapping. Such an approach may however be very sensitive to actuator delay and sliding conditions, and may therefore be limited to very slow maneuvers. In another way, [13] has proposed an open loop motion generation strategy based on differentially flatness for a general 1-trailer system, and [6] has closed the loop with a control law stabilizing the flat outputs on the reference trajectory. These approaches require however the calculation of multiple derivatives and integrations hard to estimate, and that may lead to excessively noisy values in real agricultural conditions. Numerous methods based on fuzzy logic and neural networks

have also been proposed for backing up a truck-trailer from any initial position to a loading dock, see for example [11]. Such approaches require however a large diversity of training for real-world applications, and remain mainly tested on simulated systems. Moreover, the path planning problem of specific maneuvers in headlands, all the more with a trailing implement, has rarely been considered. This problem is sometimes addressed using optimal control algorithms, designed to find optimal point-to-point trajectories for a given cost function from a wide variety of configurations, see [15]. Additionally, methods are proposed to generate first a library of maneuvers incorporating the dynamics and kinematics of the vehicle, and then perform path optimization in real-time, interconnecting the maneuvers, see [4], [5].

This paper proposes to address both path planning and control issues and is organized as follows. First, a trajectory generation strategy is presented based on primitives connected together. Next, the steering and speed controllers are considered. When the vehicle-trailer system is driving forward, the steering controller is based on a kinematic model extended with sliding parameters, as in our previous work on path following for two [9] and four [3] wheel steering vehicles. The velocity controller is based on a model predictive control approach in order to anticipate for vehicle speed variations. When the system is driving backward, a different steering controller is considered. Finally, the capabilities of the proposed algorithms are investigated through full-scale experiments.

## II. REVERSE TURN MOTION PLANNER

To easily generate reverse turns for a vehicle-trailer system, and recreate the usual trajectories performed by a farmer in headland, we propose a method based on elementary primitives (line segment, arc of circle) connected together with pieces of clothoid in order to ensure curvature continuity. Such primitive-based planning approaches are widely used in the literature using either clothoids, polynomial splines, cubic spirals or elasticas to construct non-holonomic motion. The proposed approach is well-suited to the reverse turn of a vehicle-trailer system, and allows to rapidly obtain an efficient path planning solution.

### A. Definition of an arc of clothoid admissible for the vehicle

The aim is firstly to define an arc of clothoid  $BP_1$ , see figure 3(a), feasible for the considered two-front steering vehicle presented in figure 2, in order to connect a line segment  $AB$  to a circle of radius  $R$  corresponding to the minimum curvature radius of the vehicle.

The curvature  $c$  of a clothoid varies linearly with respect to its curvilinear abscissa  $s$ , see generic equation (1) and corresponding shape illustrated in figure 3(a).

$$c = gs \quad (1)$$

Let  $c_V$  denote the curvature of the circle that the vehicle describes when orientating its wheels with a constant angle  $\delta_F$ , see figure 4(b). We clearly have:

$$c_V = \frac{\tan\delta_F}{L_1} \quad (2)$$

Injecting (2) in (1), and assuming perfect tracking (i.e.  $c = c_V$ ) leads to:

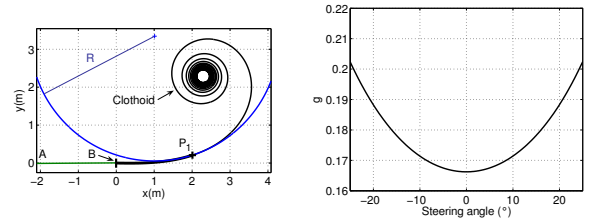
$$g = \frac{dc}{ds} = \frac{dc_V}{ds} = \frac{1}{L_1 \cos^2 \delta_F} \frac{d\delta_F}{ds} \quad (3)$$



- Max. front-wheel steering angle:  $\delta_{Fm} = 25^\circ$
- Max. front-wheel angular velocity:  $\omega_a = 20^\circ/s$
- Ref. vehicle linear velocity:  $v_{ref} = 1.75m/s$
- Max. longitudinal acceleration:  $a_m = 1m/s^2$
- Resp. vehicle and trailer wheel base:  $L_1 = 1.2m, L_3 = 2.34m$
- Vehicle tow-hitch:  $L_2 = 0.46m$

Fig. 2. Experimental vehicle-trailer system and its main parameters

Then, for the considered vehicle, a suitable proportionality coefficient  $g$  can be computed: in view of the maximum front wheel angular velocity  $\omega_a$  and of the reference vehicle linear velocity  $v_{ref}$  during the reverse turn, we have  $\frac{d\delta_F}{ds} = 0.11^\circ/cm$ . Reporting this value into (3) supplies the relation  $g = f(\delta_F)$  depicted in figure 3(b). If  $g$  is chosen as  $g_{min} = 0.166m^{-2}$ , then the arc of clothoid is admissible by the vehicle whatever  $\delta_F$ .



(a) Clothoid,  $g = 0.15$

(b)  $g = f(\delta_F)$

Fig. 3. Clothoid and computation of  $g$

To avoid the saturation of the steering actuator, this value will be reduced by 10% in the following, i.e.  $g = 0.15m^{-2}$ . For the same reason,  $R$  is chosen as  $\frac{L_1}{\tan(20^\circ)} = 3.29m$ . As presented in figure 3(a), only the arc of clothoid  $BP_1$  is performed by the vehicle until the circle of radius  $R$  is reached at  $P_1$ , corresponding to the curvilinear abscissa  $s_1 = \frac{1}{g \cdot R} = 2.02m$ . As detailed in [16] for highway design, the Cartesian coordinates of the clothoid can be written using Fresnel integrals, which can be approximated using different methods, e.g. trapezoids method or development in Taylor series. The arc of clothoid  $BP_1$  can thus be entirely defined to connect a line segment to a circle of radius  $R$ , leading to continuous curvature trajectories admissible for the vehicle.

### B. Trajectory generation strategy

The proposed strategy is depicted in figure 4(a), and consists in the following steps.

- The first movement from  $B$  to  $S_1$  is composed of an arc of clothoid  $BP_1$  to go from curvature  $c = 0$  to  $c = \frac{1}{R}$ , an arc of circle  $P_1P_2$  of center  $I_1$  and of radius  $R$ , a second arc of clothoid  $P_2P_3$  to go from curvature  $c = \frac{1}{R}$  to  $c = 0$ , and a part of a third arc of clothoid  $P_3S_1$  required to align the trailer with the vehicle at the end of the movement. Aligning the vehicle-trailer system at  $S_1$  leads to a suitable configuration to plan the reverse motion. Moreover, the path length does not vary so much w.r.t. the trailer length. In fact, for the experimental trailer (i.e.  $L_3 = 2.34m$ ),  $\overline{P_4S_1}$  is  $1.8m$ . If  $L_3$  was  $1m$  (small trailer) or  $5m$  (long trailer),  $\overline{P_4S_1}$  would only need to be respectively  $80cm$  shorter or  $90cm$  longer to align the vehicle-trailer system. Finally, at stop point  $S_1$ , the wheels are reorientated to change the vehicle instantaneous rotation center to  $I_2$ .
- The reverse movement is then built, composed firstly of an arc of circle  $S_1P_4$  to increase the vehicle-trailer angle  $\phi$  (see the notation in figure 4(b)). The point  $P_4$  has been determined by off-line preliminary simulations in order that the vehicle-trailer system reaches the configuration shown in figure 4(b) with  $\delta_F = 20^\circ$  and  $\phi = 53^\circ$ . It corresponds to the configuration enabling a circular motion of radius  $R$  when pure rolling without sliding conditions are assumed. It serves here as an objective configuration. At  $P_4$ , the wheels are reorientated to change the vehicle instantaneous rotation center from  $I_2$  to  $I_3$ . Then, an arc of circle  $P_4S_2$  of center  $I_3$  and radius  $R$  is built.
- The third movement is composed of an arc of circle  $S_2P_5$  of center  $I_3$  and radius  $R$ , and an arc of clothoid  $P_5C$  to go from curvature  $c = \frac{1}{R}$  to  $c = 0$ . The point  $S_2$  is the intersection between the circles of center  $I_3$  and  $I_4$ .

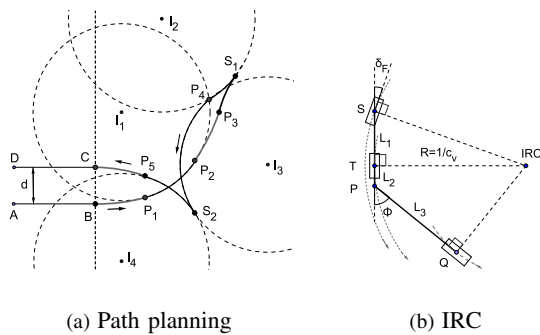


Fig. 4. Trajectory generation strategy

Figure 5 presents path planning results with two adjacent tracks separated from a distance  $d = 2m$ . The vehicle body is represented by a blue rectangle and the trailer by a red bar. At the first stop point  $S_1$ , the vehicle-trailer angle is  $\phi = 0^\circ$ , i.e. the trailer and the vehicle are aligned. The trajectories of points  $S$ ,  $T$  and  $Q$ , respectively the center of the vehicle front and rear axle and the center of the trailer axle, are shown in figure 5. During the reverse motion, the vehicle-trailer angle reaches and maintains the expected configuration  $\phi = 53^\circ$ .

In addition, speed references have to be associated at each point of the planned trajectories. They are chosen in order that the acceleration when commuting from the reference velocity  $v_{ref} = 1.75m/s$  to the approaching velocity  $v_{min} = 0.6m/s$  does not exceed the vehicle maximum longitudinal acceleration  $a_m = 1m/s^2$ . After the first stop point, the reverse motion is performed at  $-v_{min}$  until the system goes past the point  $P_4$  so that the wheels can safely be reorientated from a configuration with  $I_2$  as the ICR to the next one with  $I_3$  as the ICR.

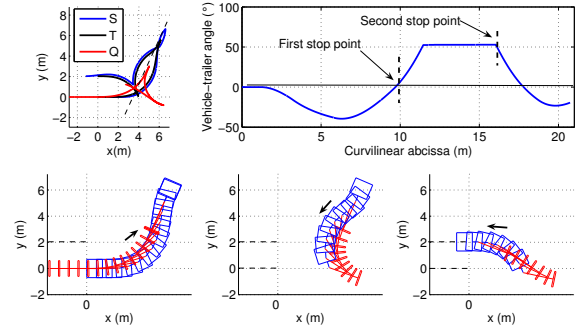


Fig. 5. Path planning results

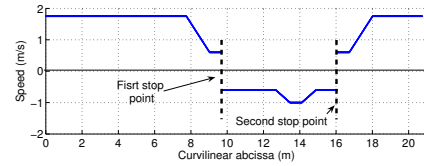


Fig. 6. Speed reference

With the motion planner presented in this section, based on geometric primitives connected together, and the associated speed reference, the reverse turn for the vehicle-trailer system is completely defined. The next section presents the control algorithms developed to accurately follow such trajectories.

### III. CONTROL ALGORITHMS

As the vehicle-trailer system is well-known for being naturally exponentially stable when driving forward, the trailer is ignored in this case, i.e. during the first and third movements of the planned motions. The associated steering and speed control algorithms are then described in subsection A. The control algorithms for the backward motion are described in subsection B.

#### A. Forward motions

Accurate automatic guidance of mobile robots in an agricultural environment constitutes a challenging problem, mainly due to the low grip conditions usually met in such a context. In fact, as pointed out [17], if the control algorithms are designed from pure rolling without sliding assumptions, the accuracy of path tracking may be seriously damaged, especially in curves. For example, [9] reports that the lateral deviation of a tractor at  $2.2m/s$  in curve can exceed  $40cm$  if the control law does not take into account the sliding phenomenon. Therefore, to perform accurate path following

and accurately stop at  $S_1$ , the low grip conditions has to be accounted in the control design.

1) *Kinematic model extended with sliding parameters:* In the same way than in [9], two parameters homogeneous with sideslip angles in a dynamic model, are introduced to extend the classical two-wheel steering kinematic model, see the bicycle representation of the vehicle in figure 7. These two angles, denoted respectively  $\beta_F$  and  $\beta_R$  for the front and rear axle, represent the difference between the theoretical direction of the linear velocity vector at wheel centers, described by the wheel plane, and their actual direction. These angles are assumed to be entirely representative of sliding influence on vehicle dynamics. The notations used in this paper are listed below and depicted in figure 7.

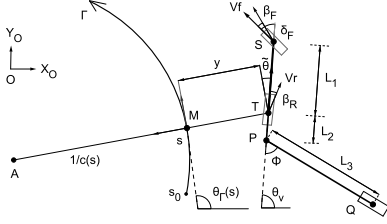


Fig. 7. Path tracking parameters

- $S$  and  $T$  are respectively the center of the front and rear virtual wheels.  $T$  is the point to be controlled.
- $\theta_v$  is the orientation of vehicle centerline with respect to an absolute frame  $[O, X_O, Y_O]$ .
- $\delta_F$  is the front steering angle and constitutes the first control variable.
- $V_r$  is the vehicle linear velocity at point  $T$  and constitutes the second control variable.
- $\beta_F$  and  $\beta_R$  are the front and rear sideslip angles.
- $M$  is the point on the reference path  $\Gamma$  to be followed, which is the closest to  $T$ .
- $s$  is the curvilinear abscissa of point  $M$  along  $\Gamma$ .
- $c(s)$  is the curvature of the path  $\Gamma$  at point  $M$ .
- $\theta_\Gamma(s)$  is the orientation of the tangent to  $\Gamma$  at point  $M$  with respect to the absolute frame  $[O, X_O, Y_O]$ .
- $\tilde{\theta} = \theta_v - \theta_\Gamma$  is the vehicle angular deviation.
- $y$  is the vehicle lateral deviation at point  $T$ .
- $\phi$  is the trailer-vehicle angle.

The equations of motion are derived with respect to the path  $\Gamma$ . It can be established, see [9], that:

$$\begin{cases} \dot{s} = V_r \frac{\cos(\tilde{\theta} - \beta_R)}{1 - c(s)y} \\ \dot{y} = V_r \sin(\tilde{\theta} - \beta_R) \\ \dot{\tilde{\theta}} = V_r [\cos(\beta_R)\lambda_1 - \lambda_2] \\ \dot{\phi} = -V_r \frac{L_2 \sin \delta_F \cos \phi + L_3 \sin \delta_F + L_1 \cos \delta_F \sin \phi}{L_1 L_3 \cos \delta_F} \end{cases} \quad (4)$$

$$\text{with: } \lambda_1 = \frac{\tan(\delta_F - \beta_F) + \tan(\beta_R)}{L_1}, \quad \lambda_2 = \frac{c(s) \cos(\tilde{\theta} - \beta_R)}{1 - c(s)y}$$

The first three equations of model (4) accurately describe the vehicle motion in presence of sliding as soon as the two

additional parameters  $\beta_F$  and  $\beta_R$  are known. An observation algorithm has been developed to achieve sideslip angles indirect estimation, relying on the sole lateral and angular deviation measurements, see [10]. This observer is based on the duality between observation and control, and is studied as a classical control problem.  $\beta_F$  and  $\beta_R$  are considered as control variables to be designed in order to ensure the convergence of the extended model outputs  $(y, \tilde{\theta})_{obs}$  to the measured variables  $(y, \tilde{\theta})_{mes}$ .

2) *Control laws design:* The extended model (4) constitutes a relevant basis for mobile robot control design. The control objective is on one hand to perform an accurate path tracking with respect to lateral and angular deviations, and on the other hand to regulate the vehicle velocity on the planned speed reference. In [9], the first three equations of model (4) have been converted in exact way into linear equations, according to the following state and control transformations:

$$\begin{aligned} [s, y, \tilde{\theta}] &\rightarrow [a_1, a_2, a_3] = [s, y, (1 - cy) \tan(\tilde{\theta} + \beta_R)] \\ [V_r, \delta_F] &\rightarrow [m_1, m_2] = \left[ \frac{V_r \cos(\tilde{\theta} + \beta_R)}{1 - c(s)y}, \frac{da_3}{dt} \right] \end{aligned} \quad (5)$$

This leads to the following chained form (6), expressed with derivatives with respect to the curvilinear abscissa:

$$\begin{cases} a_2' = \frac{da_2}{da_1} = a_3 \\ a_3' = \frac{da_3}{da_1} = m_3 = \frac{m_2}{m_1} \end{cases} \quad (6)$$

Since chained form (6) is linear, a natural expression for the virtual control law is (7):

$$m_3 = -K_d a_3 - K_p a_2 \quad (K_p, K_d) \in \mathbb{R}^{+2} \quad (7)$$

since it leads to (8), which implies that both  $a_2$  and  $a_3$  converge to zero, i.e.  $y \rightarrow 0$  and  $\tilde{\theta} \rightarrow \beta_R$ .

$$a_2'' + K_d a_2' + K_p a_2 = 0 \quad (8)$$

The inversion of control transformations provides then the following steering control law (9) for the front axle.

$$\delta_F = \beta_F + \arctan \left\{ -\tan(\beta_R) + \frac{L_1}{\cos(\beta_R)} \left( \frac{c(s) \cos \tilde{\theta}_2}{\alpha} + \frac{A \cos^3 \tilde{\theta}_2}{\alpha^2} \right) \right\} \quad (9)$$

$$\text{with: } \begin{cases} \tilde{\theta}_2 = \tilde{\theta} - \beta_R \\ \alpha = 1 - c(s)y \\ A = -K_p y - K_d \alpha \tan \tilde{\theta}_2 + c(s) \alpha \tan^2 \tilde{\theta}_2 \end{cases}$$

In addition, as the actuation delays and vehicle inertia may lead to significant overshoots, especially at each beginning/end of curves, a predictive action has been added to the steering control in order to maintain accurate path tracking performances, see [10] for more details.

As the path following performances were demonstrated to be independent from the vehicle velocity, see [9], a second control loop is therefore built, dedicated to speed control. In [2], a Model Predictive Control technique is used to anticipate speed variations and reject significant overshoots in longitudinal motion, mainly due to engine delay and inertia. The principle is that, since the speed reference at each point

of the maneuver is known, the desired value for the vehicle velocity  $D_{t+h}$  after an horizon of prediction  $h$  can be inferred from the current position of the vehicle w.r.t. the trajectory. Then, relying on the actuator model to predict the behaviour of the system, a control value  $C_t$  can be computed, with the aim that the actual velocity  $V_t$  follows an ideal reference trajectory  $\xi$  tending towards  $D_{t+h}$ .  $\xi$  is classically chosen as a first order dynamic:

$$\xi_{t+i} = D_{t+h} - (D_{t+h} - V_t) \lambda^i \quad \text{with } 0 < \lambda < 1 \quad (10)$$

The velocity actuator model was identified as a first order system, with time constant  $\tau = 0.42s$  and gain  $K = 0.97$ . The model output  $q$  at time  $t+h$ , when applying constantly control  $C_t$  from initial output value  $V_t$ , is:

$$q_{t+h} = V_t e^{-\frac{h}{\tau}} + C_t K \left(1 - e^{-\frac{h}{\tau}}\right) \quad (11)$$

Therefore, from (10) and (11), the control value  $C_t$  ensuring  $q_{t+h} = \xi_{t+h}$  is deduced :

$$C_t = \frac{[D_{t+h} - V_t] (1 - \lambda^h) + V_t \left(1 - e^{-\frac{h}{\tau}}\right)}{K \left(1 - e^{-\frac{h}{\tau}}\right)} \quad (12)$$

### B. Backward motion

During the backward motion, the previous steering control law (9) can be used until the vehicle-trailer system presents an angle  $\phi_{ref} = 53^\circ$ , corresponding to the configuration at point  $P_4$  depicted in figure 4(b).

Next, as the rest of the backward movement is relatively short to reach the stop point  $S_2$ , it is proposed to stabilize the vehicle-trailer angle on  $\phi_{ref}$ . This solution has the advantage to be easy to implement, and avoid the difficulties commonly met when stabilizing vehicle-trailers on a trajectory in backward motion in high sliding conditions. Relying on the fourth equation of model (4), the error dynamic  $\dot{\phi} = K_R(\phi_{ref} - \phi)$  (with  $K_R > 0$ ) can then be imposed with the following front-wheel steering control law:

$$\delta_F = \arctan \frac{-L_1 \sin \phi - \frac{K_R L_1 L_3 (\phi_{ref} - \phi)}{V_r}}{L_2 \cos \phi + L_3} \quad (13)$$

The speed control law for the backward motion is unchanged w.r.t. the forward motion.

## IV. EXPERIMENTAL RESULTS<sup>1</sup>

In this section, capabilities of the proposed control algorithms are investigated on an irregular natural terrain composed of mud and wet grass, using the experimental two-wheel steering mobile robot and trailer depicted in figure 2. The only exteroceptive sensor on board is an RTK-GPS receiver, whose antenna has been located straight up the center of the vehicle rear axle. It supplies an absolute position accurate to within 2cm, at a 10Hz sampling frequency. The vehicle-trailer angle is measured using potentiometers depicted in the right bottom part of figure 2. A gyrometer is also used to obtain an accurate heading of the vehicle

during the maneuvers. In the forthcoming experimental test, the objective for the vehicle-trailer system is to follow autonomously two straight lines  $AB$  and  $CD$ , separated from  $2m$ , and to execute also autonomously the reverse turn, see figure 8(a). The lateral deviation recorded at the center  $T$  of the rear wheels, according to the curvilinear abscissa, is reported in figure 8(b).

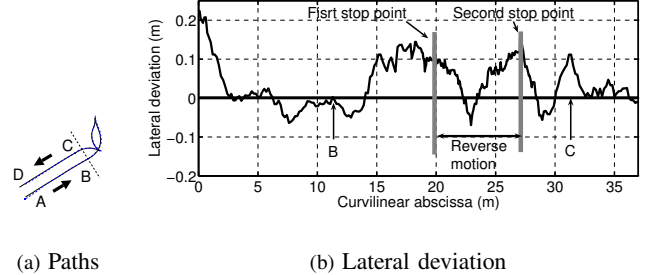


Fig. 8. Experimental results

At the beginning, the vehicle starts at about  $25cm$  from the path to be followed. Then, it reaches the planned path and maintains an overall lateral error about  $\pm 15cm$  in spite of a fast speed on an irregular soil. A thorough analysis establishes that the main overshoots on the lateral deviation take place mainly when the vehicle goes out of the curves at full speed (curvilinear abscissas  $15m$  and  $32m$ ). In fact, although the use of predictive action allows to significantly reduce such overshoots, the fast variation in the sliding conditions may drive the tires to lose lateral stability and the vehicle drifts towards the outside of the curve. Therefore, the sideslip angle observer needs to be more reactive. This may demand the integration of dynamic features (location of the center of gravity, moments of inertia, ...) into the observer algorithm, in order to decrease estimation delays and improve accuracy at such transient phases. That point will be investigated in future development.

The vehicle speed w.r.t. the curvilinear abscissa is reported at the top of figure 9. At the bottom of figure 9 is also reported the vehicle front steering angle.

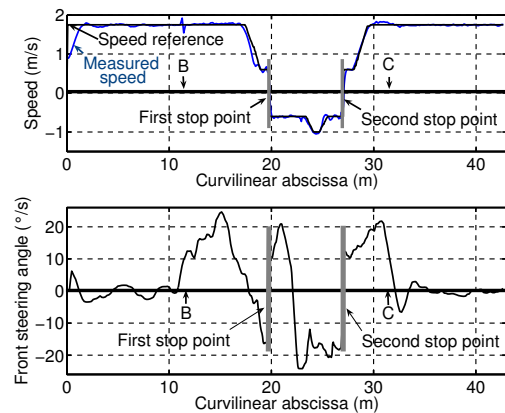


Fig. 9. Speed and front steering angle

The velocity  $v_{ref} = 1.75m/s$  is correctly followed. The speed variations are satisfactorily anticipated with the pre-

<sup>1</sup> A video of this experiment can be found on the Cemagref FTP server <ftp://ftp.clermont.cemagref.fr/pub/ArocoRq>

dictive approach. It can also be observed that the variations of the front steering angle are quite smooth and that the wheels are reorientated to change the vehicle instantaneous rotation center at the stop points. At curvilinear abscissas  $15m$  and  $32m$ , the steering angle reaches  $25^\circ$  to counteract the overshoots in the lateral deviation.

The vehicle-trailer angle w.r.t. the curvilinear abscissa is reported in figure 10. In accordance with the simulations depicted in figure 5, this angle reaches  $-40^\circ$  during the first movement. The trailer and the vehicle are then aligned at the first stop point. During the reverse motion, this angle increases until  $\phi = 53^\circ$ . The slight overshoot at curvilinear abscissa  $22m$  is due to the duration of the change in vehicle instantaneous rotation center from  $I_2$  to  $I_3$ . The angle is then well-regulated to the value  $\phi = 53^\circ$ .

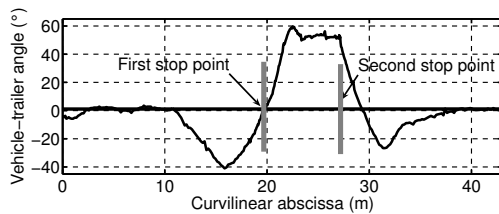


Fig. 10. Vehicle-trailer angle

These results show that the planned motions obeying vehicle's kinematic and dynamic constraints, together with sliding estimation and lateral/longitudinal controllers with predictive actions, enable to obtain satisfactory path following results for an off-road mobile robot pulling a trailer, even during backward maneuvers.

## V. CONCLUSION AND FUTURE WORK

This paper addresses the problem of path generation and motion control for the autonomous maneuvers of a farm vehicle with a trailed implement in headland. A reverse turn path planning algorithm is firstly presented. The trajectories are built using elementary primitives (line segment, arc of circle) connected together with pieces of clothoid in order to ensure curvature continuity. Next, the steering and speed controllers are presented. When the vehicle-trailer system is driving forward, an extended kinematic model accounting for sliding effects via two additional sideslip angles is considered. This model is used to derive a steering control algorithm independent from the vehicle velocity. A second control loop dedicated to vehicle speed control is used, based on model predictive algorithm to anticipate speed variations and compensate for low-level characteristics. When the system is driving backward, a different steering controller is considered aiming at controlling the vehicle-trailer angle.

Promising results are presented with an off-road experimental mobile robot pulling a trailer during a reverse turn maneuver. In spite of fast speed and steering variations required to perform such a maneuver, an overall tracking error within  $\pm 15cm$  is obtained. More accurate path following performances could be obtained using a more reactive

sideslip angle observer. This last point is the object of further development based on the design of a mixed kinematic and dynamic observer.

This system could also be advantageously coupled with a device performing repetitive actions on a farm vehicle, such as the control of the hitches, the power take-off and the hydraulic valves, in order to relieve the human driver of such tasks tedious to perform during headland turns, and then obtain a full automated solution. Furthermore, the execution of such maneuvers with a four-wheel steering vehicle and trailer is currently also investigated to take advantage of explicitly controlling both lateral and angular deviations (see first developments on the path following task in [3]).

## REFERENCES

- [1] Altafani C., Speranzon A., Wahlberg B. *A feedback control scheme for reversing a truck and trailer vehicle*. In IEEE Transactions on robotics and automation, 17:915-922, December 2001.
- [2] Cariou C., Lenain R., Thuilot B., Martinet P. *Motion planner and lateral-longitudinal controllers for autonomous maneuvers of a farm vehicle in headland*. In IEEE International conference on Intelligent Robots and Systems, St Louis, USA, October 11-15 2009.
- [3] Cariou C., Lenain R., Thuilot B., Martinet P. *Adaptive control of four wheel steering off road mobile robots: application to path tracking and heading control in presence of sliding* In IEEE International conference on Intelligent Robots and Systems, Nice, France, September 22-26, 2008.
- [4] Egerstedt M., Koo T. J. *An integrated algorithm for path planning and flight controller scheduling for autonomous helicopters* In 7th Mediterranean conf. on control and automation, Haifa, Israel, 1999.
- [5] Frazzoli E., Dahleh M. A., Feron E. *Maneuver-based motion planning for nonlinear systems with symmetries* In IEEE Transactions on robotics, 21(6), 2005.
- [6] Hermosillo J., Sekhavat S. *Feedback control of a bi-steerable car using flatness: application to trajectory tracking*. In IEEE International American Control Conference, 4:3567-3572, 2003.
- [7] Katupitiya J., Eaton R., Yaqub T. *Systems engineering approach to agricultural automation: new developments* In IEEE Systems Conference, Honolulu, Hawaii, USA April 9-12 2007.
- [8] Lamiroux F., Laumond J.P. *A practical approach to feedback control for a mobile robot with trailer*. In IEEE International conference on Robotics and Automation, Louvain, Belgique, 3291-3296, May 1998.
- [9] Lenain R., Thuilot B., Cariou C., Martinet P. *High accuracy path tracking for vehicles in presence of sliding. Application to farm vehicle automatic guidance for agricultural tasks* Autonomous robots, 21(1):79-97, 2006.
- [10] Lenain R., Thuilot B., Cariou C., Martinet P. *Adaptive and predictive path tracking control for off-road mobile robots* European journal of control, 13(4):419-439, 2007.
- [11] Park J.I., Cho J.H., Chun M.G., Song C.K. *Neuro-fuzzy rule generation for backing up navigation of car-like mobile robots*. Journal of Fuzzy Systems, 11(3), 2009.
- [12] Pedersen S.M., Fountas S., Have H., Blackmore B.S. *Agricultural robots - system analysis and economic feasibility* Precision Agriculture, 7(4):295-308, 2006.
- [13] Rouchon P., Fliess M., Levine J., Martin P. *Flatness, motion planning and trailer systems*. In IEEE International conference on Decision and Control, San Antonio, TX, USA, 3:2700-2705, 1993.
- [14] Tilbury D., Sordalen O., Bushnell L., Sastry S. *A multi-steering trailer system: conversion into chained form using dynamic feedback*. In IEEE Transactions on robotics and automation, 11(6):807-818, 1995.
- [15] Vougioukas S., Blackmore S., Nielsen J., Fountas S. *A two-stage optimal motion planner for autonomous agricultural vehicles*. Precision Agriculture, 7:361-377, 2006.
- [16] Walton D.J. *Spiral spline curves for highway design*. Microcomputers in civil engineering 4:99-106, 1989.
- [17] Wang D., Low C. B. *Modeling skidding and slipping in wheeled mobile robots: control design perspective*. In Proc. of the IEEE int. conf. on Intelligent Robots and Systems, Beijing, China, Oct 2006.